Mass Transit Power Traction Networks as Communication Channels

Pavels Karols, Klaus Dostert, *Senior Member, IEEE*, Gerd Griepentrog, and Simon Huettinger

***Abstract*—The rapid progress of power line communications (PLC) for data transmission over electric power supply systems is now opening ways for special applications such as train automation in local transportation and mass transit (MT) systems. These DC-powered traction networks can be used as communication links between wayside equipment and the moving trains. As MT networks significantly differ from usual electricity supply systems, the usage of existing models and communication equipment for conventional PLC channels turns out infeasible. Therefore, the work reported in this paper focuses on MT channel investigation and modeling, in order to develop novel adapted solutions. The outcome is a stochastic MT channel model, which—besides multipath and time-variance—also includes peculiar properties such as the behavior of ring structures and the impact of the Doppler effect invoked by moving trains. In addition, a very special interference scenario is treated, caused by the rectifiers in these DC-powered environments.**

Besides a complete simulation model, this paper presents detailed guidelines for building emulation hardware, so that channel adapted PLC system design for MT networks can now be successfully started without further expensive field trials.

***Index Terms*—Channel modeling, mass transit (MT), multipath channel, power line communication (PLC), power traction networks, time-varying fading channel, ultra-wideband channel.**

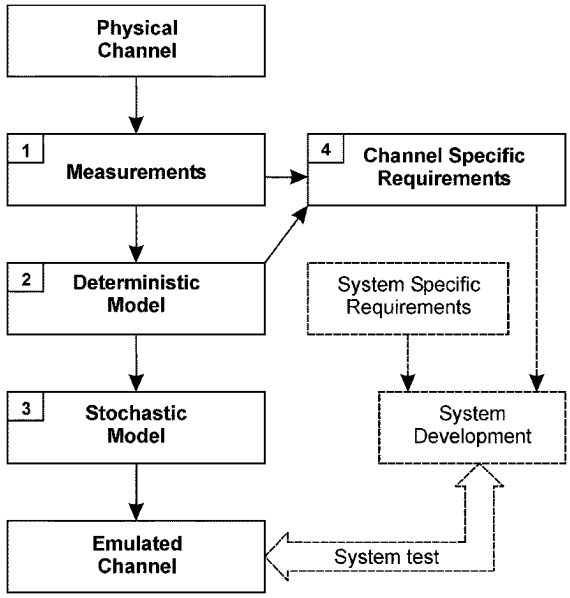

Fig. 1. General modeling concept.

I. Introduction

THE CAPACITY OF modern transportation systems is measured in train course intervals and depends essentially on the deployed train control system. To facilitate efficient automatic train operation and protection in mass transit (MT), bidirectional communication between fixed wayside equipment and mobile equipment onboard the train is necessary. Due to the availability of power traction lines at every location within a railway network, there is great interest to use these lines as communication medium [1].

To ensure the required quality-of-service and utilize the channel close to its capacity, channel-adapted communication systems are needed. For this purpose, channel investigations are necessary as a first step. In this context, the low-frequency ranges up to 148.5 kHz in Europe and to 500 kHz in America and Asia [2] are of special interest, as regulations for their use exist in form of CENELEC EN50065 (Europe) and, e.g., corresponding FCC rules in USA. Unfortunately, the current literature does not provide any inside into low-frequency properties of power traction networks in MT. Up to now, the characteristics of such networks were obviously not examined. Consequently, concepts of channel-adapted communication systems could not be proposed. The driving force behind the work presented here is the need to explore the channel properties and to develop a new wideband channel model with a corresponding simulator for widespread 750 VDC traction networks. Fig. 1 depicts the general concept of channel exploration, which will be developed and applied in the following. As Fig. 1 indicates, there are four basic portions which will be described throughout this paper.

In order to evaluate potential limits and fundamental properties of MT-PLC channels some investigations and estimations of the channel characteristics beyond theoretical considerations are necessary. Section II outlines the results of an accomplished measuring campaign. In the second step, due to the complexity of measurements, a deterministic channel model was developed for detailed understanding of channel behavior under controlled conditions. This is reviewed in Section III. Then, based on the results of deterministic modeling, a stochastic model was developed and is discussed in Section IV. This model is useful for channel simulation and emulation, which both are recognized as effective means to evaluate communication system performance. Especially, emulation provides the capability of sophisticated testing in a laboratory environment under real-time

Manuscript received April 21, 2005; revised December 7, 2005 and February 23, 2006. This work was supported in part by Siemens Transportation Systems.

P. Karols, G. Griepentrog, and S. Huettinger are with the Siemens AG Corporate Technology, D-91058 Erlangen, Germany (e-mail: pavels.karols@siemens.com; gerd.griepentrog@siemens.com; simon.huettinger@siemens.com).

K. Dostert is with the University of Karlsruhe, D-76187 Karlsruhe, Germany (e-mail: klaus.dostert@iiit.uni-karlsruhe.de).

Digital Object Identifier 10.1109/JSAC.2006.874410

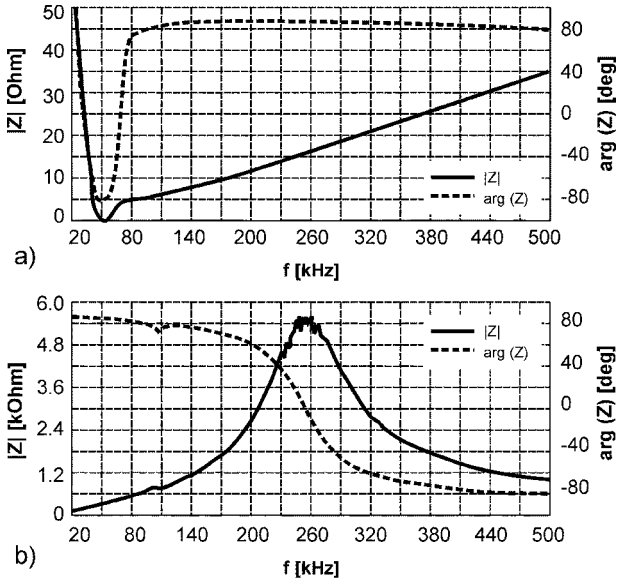

Fig. 2. Absolute value and phase. (a) Train without choke. (b) Train choke.

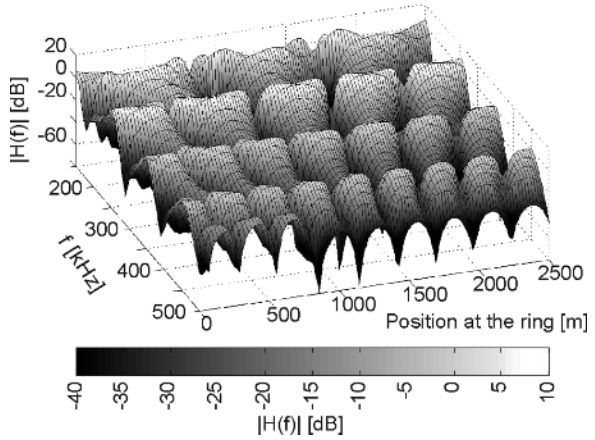

Fig. 3. Example of the transfer function at a ring structure, dependent on position.

constraints. Eventually, Section V is dedicated to the analysis of channel-caused requirements for system design. The goal of this section is to exploit opportunities to adapt communication system parameters to channel properties and to improve overall system performance.

II. Measurements

A. Network Conditioning

In this section, first the characteristic impedances of different network components such as vehicles, electrical rectifiers, and access impedance values are presented. Since power supply networks are in principle not conceived for the transmission of high frequencies, they will normally exhibit bad transmission characteristics [2].

According to measurements performed for different network components [2], [22], it was asserted that access impedances are generally much lower than the characteristic impedance of the traction line (approximately 250 Ohms). Typical values are found in the range down to 30 Ohms inductive [Fig. 2(a)]. This mismatch causes high values of the voltage standing wave ratio (VSWR) along the line and calls for equipping transmitters with low output impedance, boosting the injected signal power.

To simplify the requirements for measurement equipment and future data transmission systems and to improve transmission characteristics of the channel, it appears rewarding to examine possibilities of network conditioning. Toward this aim, chokes were installed in series with the power circuits. Unfortunately, the entire traction current has to pass such a choke reaching values up to some thousand ampères. Thus, strong premagnetization or even saturation occurs. Coreless coils are therefore preferred to avoid the nonlinear effects of possible saturation. To increase the inductance of coreless coils, a rather high number of turns is needed. This leads to parasitic capacities between the turns and neighboring pieces of metal, so that resonances occur at certain frequencies. Above such a resonant frequency the choke does no longer represent an inductor, but has turned into a capacitor.

On the market there are standard chokes available, which have been designed for high traction currents. The documentation of such devices, however, does not provide any information about high-frequency properties, so that corresponding investigations are required. The measuring system developed and used in the following is based on separating forward and reflected waves. Fig. 2(b) depicts the example of a choke used for the measurements in the form of a coreless coil with 1 mH of nominal inductance. Note that the impedance does not increase linearly with frequency and takes on capacitive character, as expected, above the resonance frequency at approximately 250 kHz. In the observed frequency range, the chokes offer an increase of access impedances up to some 100 Ohms. Thus, the influence of moving trains on signal propagation is minimized and the VSWR value essentially decreases.

B. Transfer Function

To investigate the transfer characteristics of an MT-PLC channel, a further method based on sinusoidal signals was developed and applied within the frequency range from 50 up to 500 kHz [2]. The measurements were accomplished at the SIEMENS track test center in Wildenrath (Germany). The test installation reproduces a real rail traction network with an overhead catenary line, but nevertheless, it features some peculiarities, which influence signal propagation. The installation's topology is a ring structure with a total length of approximately 2500 m. Furthermore, a single branch of approximately 400 m with an open end is attached to the ring [2]. Fig. 3 shows a measured example of the transfer function dependent on the position at the ring and the frequency over a range from 50 up to 500 kHz.

As Fig. 3 clearly indicates, the employed test installation intensifies the wave propagation effects, as waves obviously circulate several times, generating distinct fluctuations of the amplitude along the ring. Depending on the used frequencies, amplitudes may locally even exceed the value of the transmitter's output signal (Ferranti Effect), while almost total

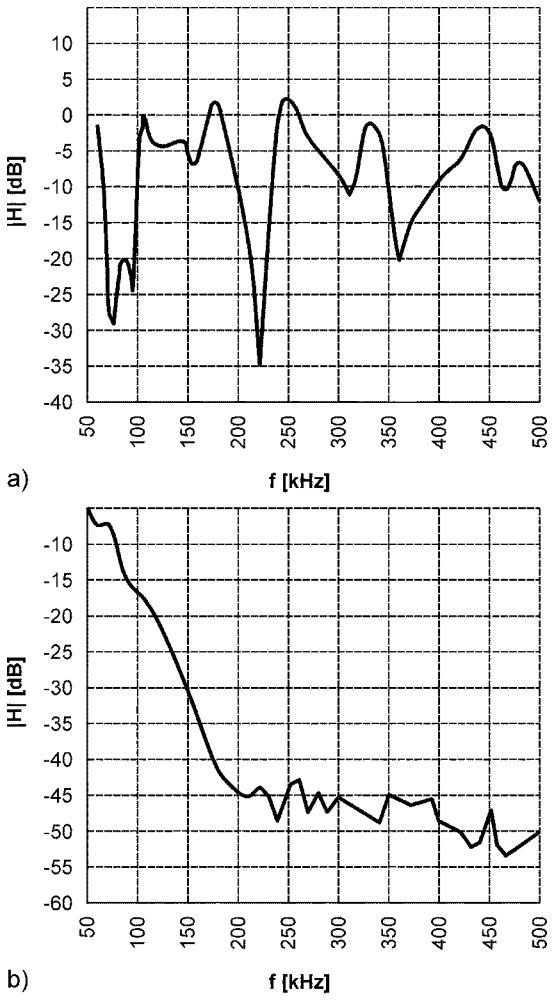

Fig. 4. Attenuation of sinusoidal signals along the test line. (a) 100 m from the transmitter. (b) 2200 m from the transmitter.

cancellation occurs in other places. In addition, it can be recognized in Fig. 3 that the position-dependent transfer function exhibits a pronounced symmetry, which can be explained with the ring structure. For some frequencies, however, the graph becomes unsymmetrical. This is caused by the mentioned branch, which introduces a frequency-dependent access impedance.

In Fig. 4, the amplitude responses at different positions along the ring are presented. In parts of the frequency range, the attenuation reaches very high values, while the center frequency and the width of the attenuated region may differ. Fig. 4(a) shows a characteristic course with strongly pronounced attenuations. The notch widths of some kilohertz are typical for a set of measurements.

In Fig. 4(b), a further example with a greater distance of approximately 2200 m is presented. Here, low-pass behavior can be recognized. Due to losses in the conductors, the signal attenuation depends on the distance between transmitter and receiver. The low-pass characteristic is caused by the skin effect, i.e., line losses increase with the square root of frequency. Toward higher frequencies the notches "blur" more and more, since the reflected waves are stronger attenuated due to their longer propagation path.

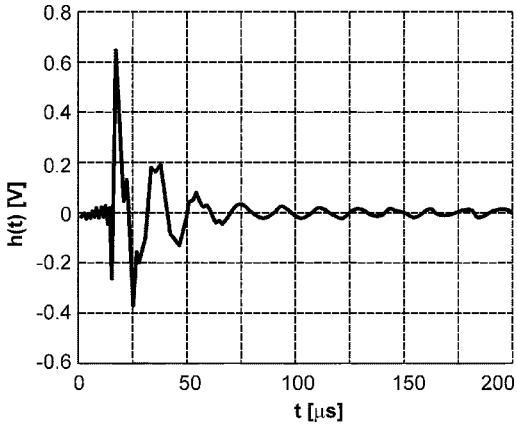

Fig. 5. Example of a channel impulse response.

C. Impulse Response

Besides the transfer function, also the impulse response of the channel is important for the development of future communication systems. Fig. 5 shows a typical example of an impulse response taken at an arbitrary location of the ring. Here, the echo behavior or the delay spread is visible. The channel exhibits received signals arising from a sum of numerous time-variant paths. The result of the superposition of different signal portions is depending on their individual phase and amplitude constellations, as well as on the location of the receiver. Generally, time dispersion and frequency selectivity are observed. According to Fig. 5, the impulse response is fading away after approximately 80–100 μs.

D. Noise Scenario

The aim of this section is to provide basic knowledge about the noise scenario in the frequency range from some 10 up to 500 kHz with the focus on impulsive noise. According to its properties, additive noise can be classified into four groups.

1) Colored background noise. It has a relatively low-power spectral density (psd), varying with frequency and is caused by summation of numerous noise sources with low power.
2) Narrowband noise. It emerges in form of discrete lines in the spectrum. This type of noise is mainly caused by spectral repetitions of high-power low-frequency disturbances introduced by nonlinearities of power supply components. A further reason for narrowband noise in the frequency range above 148.5 kHz is ingress of long wave broadcast stations.
3) Nonperiodic impulsive noise. Its casual nature is caused by switching transients within the network.
4) Periodic impulsive noise. The according impulses have repetition rates of 150, 300, or 600 Hz. Periodic impulsive noise is caused by switching transients in rectifiers at traction substations. The psd can reach values of more than 40 dB above the background noise.

Fig. 6 shows a superposition example of all types of noise in the frequency domain. The background and narrowband noise usually remain stationary over periods of seconds and minutes, or even for hours. During the occurrence of impulses, the psd of

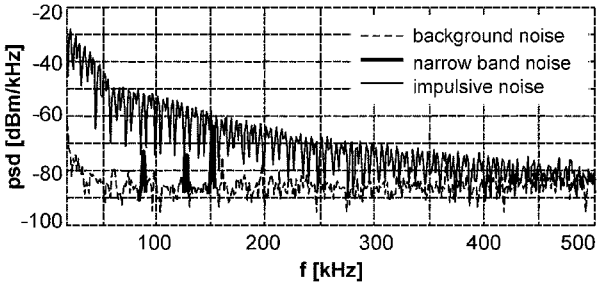

Fig. 6. Superposition of noise.

the noise is distinctly higher. As impulsive noise is generally a major source of problems for data transmission, it will be discussed here in more detail.

1) Impulsive Noise: The dominant source of this kind of noise is found at the electric rectifiers in traction substations. A rectifier for a standard three-phase AC system consists of six diodes or thyristors and performs six commutations within one period of the three-phase mains voltage. In order to reduce the ripples of the output voltage of the rectifier, several six-pulse rectifiers can be connected in parallel. DC voltage is supplied by different diodes depending on the phase position of the mains voltage. The circuit of each diode basically consists of the transformer leakage inductance and the inductance of the relatively long cables between railroad line and rectifier. Switching the current leads to carrier storage effects. Due to high currents, together with rather fast switching, the induced voltages are considerable. In measurements voltage peaks up to some 100 Volts were identified. It must be noted that this kind of impulsive noise is, however, only present as long as traction current is drawn from the rectifier.

Based on a simple physical interpretation of impulsive noise the so-called impulse rate can be derived as

$$t_{\mathrm{imp.rate}} = \frac{T_B}{N_{\mathrm{Imp}}}. \tag{1}$$

The impulse rate (1) results from a number of impulse events N_{Imp}, which arise during one period of mains voltage T_B. It describes the average time interval between consecutive impulses. The 6-, 12-, and 24-pulse rectifiers are typically used in public transportation traction power supplies. According to (1), the impulse rates are 3.333, 1.667, and 0.833 ms, respectively.

2) Impulse Noise Jitter: It was ascertained by measurements that noise impulses generally do not precisely fit into the time pattern according to (1). If the supply voltage amplitudes of the different phases are not equal, e.g., due to asymmetry of transformers and different voltage drops, there is a dispersion with respect to time, called impulse jitter in the following. Fig. 7(a) illustrates this effect in more detail. The average value of impulse jitter is, however, close to zero.

In the histogram of Fig. 7(b), it can be seen that the jitter is spread over an interval of approximately ± 80 μs. Fig. 7(b) shows as well the approximation of the histogram by means of Gaussian distributions. If the jitter events at each phase are considered as Gaussian distributed, the distribution of their sum fits almost perfectly with the measured histogram.

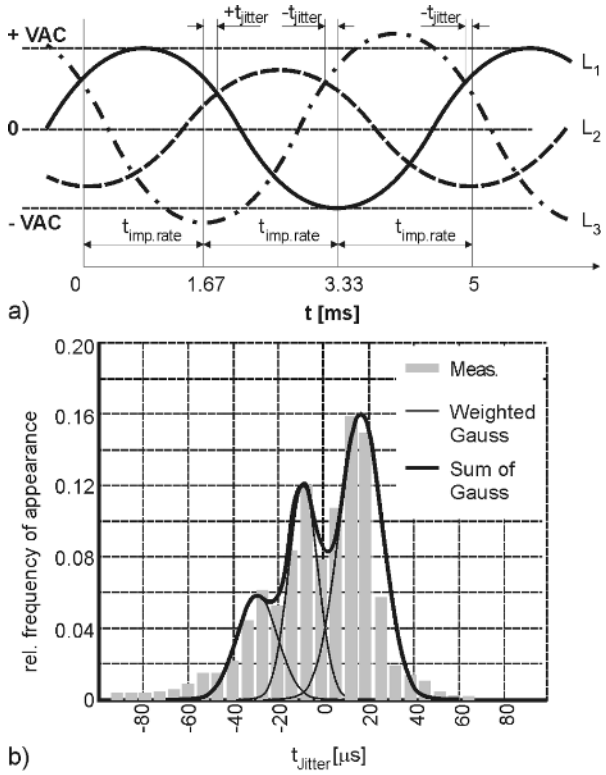

Fig. 7. Impulse jitter: (a) Physical interpretation. (b) Histogram.

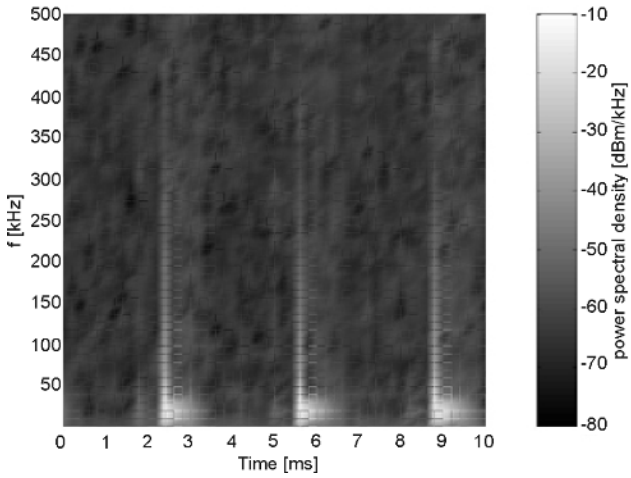

Fig. 8. Time-frequency analysis of impulsive noise.

3) Time-Frequency Analysis: To understand the dynamics of transient processes with impulsive noise in more detail, a time-frequency analysis is performed. Since the effective disturbance, which essentially corresponds to the duration of an impulse, is always much smaller than the time interval between impulses, it will be interesting to study the behavior of the noise power density between impulses. Toward this aim, in Fig. 8, the result of a time-frequency analysis based on a short-time Fourier transform with a time resolution of 205 μs is depicted. Regions with high instantaneous power density are represented with bright colors, while those with low-power density have dark colors.

The appearance of impulses within a 3.333 ms pattern, due to a six-pulse rectifier, is clearly observable. It is important to note that the analyzed impulses exhibit wideband character at the moment of their appearance, i.e., a frequency range up to 350 kHz is disturbed. The maximum impulse power density reaches −20 dBm, and thus exceeds the background noise by approximately 30–40 dB [22]. The intensity of the disturbance at higher frequencies decreases, however, rapidly with time. Solely the range below 50 kHz remains strongly disturbed over the entire duration of an impulse. Hence, in the range of low frequencies, uncritical low-level background noise is present only between impulses, while for higher frequencies the intervals, which can be assumed to be free of impulsive disturbance, are even larger. These important properties of periodic impulsive noise can be effectively used for PLC system design, as shown in Section V.

III. Deterministic Model

Since a measurement-based channel analysis requires tremendous effort, including extended observation intervals and the selection of numerous different locations, a model-based concept is developed here, in order to derive a physically motivated, deterministic channel description, not neglecting realistic conditions. Toward the model development, the following tasks have to be performed.

- Evaluation and explanation of measurement results.
- Description of new, arbitrary network structures without measurements.
- Optimization of network conditioning measures.
- Prediction of propagation conditions already in the planning and design phase of a communication system.
- Derivation of statistical parameters of a time-variant MT-PLC channel.

For the following computations, a mathematical theory based on scattering parameters of n-terminal networks is chosen, which is well known from high-frequency microwave technology [3]. For appropriate simulation of signal propagation close to reality, all network components have to be included into the model by their access impedance. The necessary impedance values are accomplished by measurements. Traction substations, line sections, line terminators, communication equipment, and all kinds of consumers, which may contribute to terminating impedance, were examined during an extended measurement campaign. The characteristic impedance of the power supply line is theoretically derived from physical parameters and geometrical dimensions, whereby overhead lines as well as "third rail systems" are considered separately.

In this manner, the complete structure of a railway system is obtained by combining components appropriately in the model. Eventually, voltages and currents of data transmission signals can be computed at any location within the network.

To evaluate computation results, they are first compared with measured data. As can be seen in [22], the calculated results show excellent agreement with the measured data.

A. Derivation of Statistical Parameters

Fig. 3 shows the typical amplitude fluctuation effects as a function of position and carrier frequency. A train is always moving through such an "interference pattern" with a certain speed. From a receiver's point of view, the fluctuations of the received amplitude may be observed as a function of time and can be modeled by a stochastic process. From literature, the phenomenon is known as "fast fading" [6]. The fading rate depends on the speed of the train and on the carrier frequency. Hence, with respect to mobile transceivers onboard moving trains, MT-PLC channels exhibit time variance, time dispersion, as well as frequency-selective fading effects.

A very practical and approved mathematical description technique involves a statistical characterization in terms of correlation functions, since the knowledge of such functions allows a determination of the channel output's autocorrelation behavior [5]. Because of the dual nature of the channel, a two-dimensional (2-D) complex time-frequency correlation function denoted as

$$R_{HH}(f_i, f_j, t_i, t_j) = E\left[H^*(f_i, t_i)H(f_j, t_j)\right] \tag{2}$$

is involved [4]–[6], where $H(f,t)$ is a time-variant transfer function.

Based on (2), two further correlation functions can be derived, namely, a frequency correlation function and a time correlation function. According to [5], the power delay profile, Doppler power density, and amplitude distribution completely describe the statistical properties of a communication channel. In the following, these key parameters are discussed.

1) Power Delay Profile and Coherence Bandwidth: An MT-PLC channel is characterized by its transfer function which varies in a more or less random fashion with frequency. Approximate constant amplitudes and phases can only be observed over sufficiently small frequency intervals. Frequency-selective fading, which may occur, will be, on one hand, highly correlated for closely spaced frequencies, and on the other, definitely uncorrelated for frequencies far apart.

As we can see from measurements [2], the fading rate over time (some seconds) is much longer than the supposed duration of transmitted signals (some milliseconds). Hence, within certain time intervals the channel can be approximated as "flat" with respect to time. Assuming the channel's impulse response to be time-invariant (in relation to the duration of transmitted signals) the complex correlation function (2) becomes

$$E\left[H(f)H(f+\Omega)\right] = q(f, \Omega) \tag{3}$$

where $H(f)$ is a time-invariant channel transfer function.

In Fig. 9, one typical example of a frequency correlation function is illustrated, based on computations with a deterministic model. When the correlation $q(f, \Omega)$ is close to its maximum $q(f, 0)$ for all $\Omega < B_c$, then all transmitted frequencies within B_c will be received fading in a highly correlated fashion. B_c is called coherence bandwidth, and generally defined as the frequency span for which $q(f, \Omega)$ exceeds 1/2 of its maximum. Computations with the deterministic model suggest a value of about 20 kHz for B_c at typical MT-PLC channels. An important consequence of this result for PLC system design is, that the coherence bandwidth can be assumed as constant over the whole decade of frequencies between 50–500 kHz.

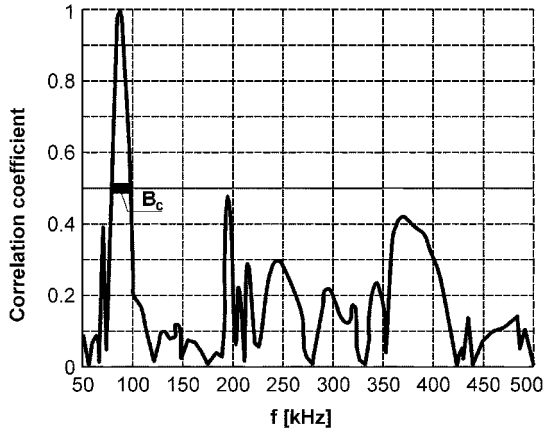

Fig. 9. Frequency correlation function for f $= 80$ kHz.

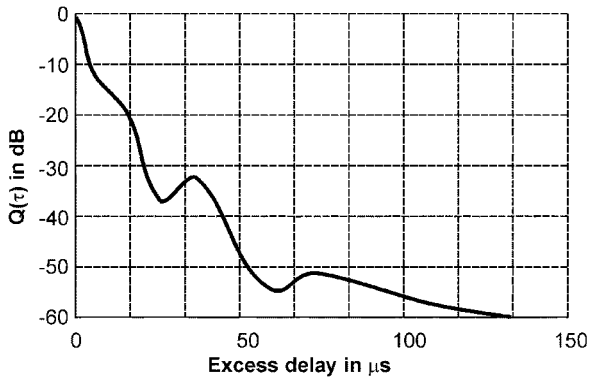

Fig. 10. Power delay profile.

Note that the channel delay spread is the reciprocal of the coherence bandwidth, due to the Fourier transform relationship between power delay profile and frequency correlation function. The power delay profile $Q(\tau)$ describes the average power of a transmission signal with time delay τ in the channel's multipath environment. One may define a delay spread parameter T_h as the width of $Q(\tau)$. Fig. 10 shows a typical power delay profile, which is calculated using the deterministic model.

Based on the properties of the frequency correlation function one may summarize the following properties of a so-called narrowband transmission channel, for which the bandwidth is smaller than the coherence bandwidth:

- attenuation within a narrowband channel is approximately constant for all frequencies;
- the phase within a narrowband channel is approximately linear;
- the fading within a narrowband channel is highly correlated for all frequencies.

2) Doppler Power Density: An MT-PLC channel has a time-variant nature. An approximately constant amplitude and phase can only be observed over finite-time intervals. The fading which occurs at some frequencies within the coherence bandwidth will remain nearly constant, that is, highly correlated for closely spaced time instants, and definitely uncorrelated for time instants sufficiently apart.

For each narrowband fading channel, being selective only with respect to time, the complex correlation function (2) becomes

$$E[H^*(f,t)H(f,t+\tau)] = R(f,\tau) \tag{4}$$

where $R(f,t)$ is called time correlation function. Here, one may define the coherence time parameter T_c in terms of $R(f,\tau)$ in the same way as B_c was defined in terms of $q(f,\Omega)$. The channel parameter T_c is then a measure of the average fade duration (fading rate) and is particularly useful in predicting the occurrence of time-selective fading in the channel and for adaptive equalizing within a communication system.

Note that the Fourier transform of a time correlation function provides the Doppler power density spectrum [6], [8]. Whenever a Doppler effect is observed, it is evident that the channel is time-variant. The time variations can be related directly to the motion of communication devices. Moreover, the Doppler shift is also time-variant, since a train's velocity may be changing. Measurements and analysis with the deterministic model confirmed, that in our context, the typical assumptions, which are well known from mobile radio channel modeling, are unfortunately not applicable.

First, an important difference between MT-PLC channels and mobile radio channels is, that in case of MT-PLC, only two directions of signal arrival are possible. The Doppler spectrum is not isotropic, since scattering behind the receiver (seen from the transmitter's location) is higher attenuated than signal portions, which did not cross the receiver's connection point.

Fig. 11 shows typical Doppler power densities for different carrier frequencies. In order to approximate the complete Doppler power density spectrum, a sum of two weighted Gaussian distributions is quite appropriate. Similar results have been obtained in radio channel measurements, where propagation along streets, forming dominant paths, was measured. This phenomenon is called *canyon effect* and has led to the definition of Gaussian spectra in COST specifications [14].

A further important insight is, that Doppler spectra are depending on the used carrier frequencies. The Doppler frequency D_K at the maximum of a Doppler spectrum becomes higher the higher the selected carrier frequency is. This leads to different amplitude fading rates. Moreover, the Doppler frequency grows linearly with increasing carrier frequency. Hence, the typically used narrowband assumption when modeling mobile radio channels—saying that the bandwidth is much smaller than the value of the carrier frequency—is clearly violated. This special property of MT-PLC channels must be taken into consideration when developing the simulation model which is proposed in the next section.

3) Amplitude Distribution: To evaluate the amplitude distribution some computations were carried out for different network structures with one or more vehicles on the line. If there are many scattering points, the amplitude distribution tends toward a Rayleigh distribution [6], which is completely characterized by mean value and standard deviation. The investigations in [22] confirm the assumption that fading on MT-PLC channels can be described with a Rayleigh distribution.

IV. Simulation Model

For the purpose of convenient communication system testing and the comparison, e.g., of different modulation schemes, an

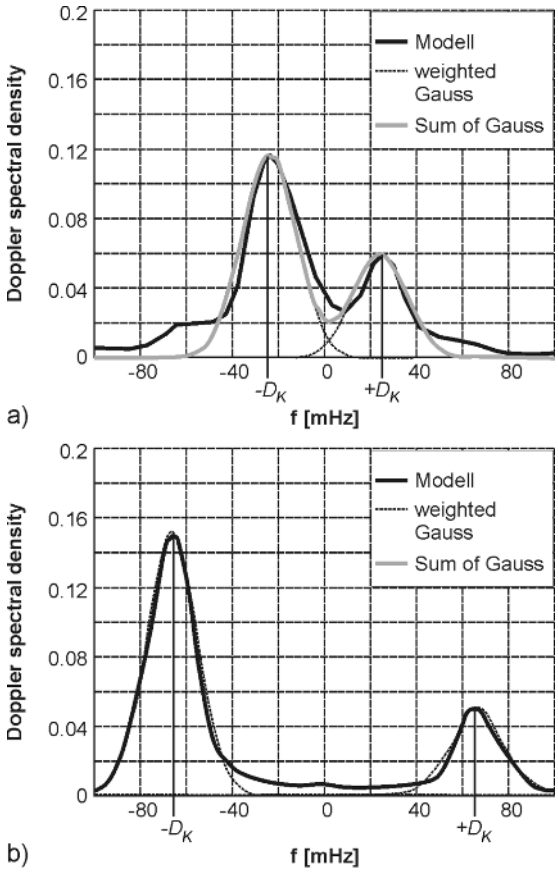

Fig. 11. Doppler power density at 150 km/h: (a) for 150 kHz; (b) for 500 kHz.

MT-PLC channel emulator is highly desirable. Such an emulator must—besides other more conventional features—include the emulation of highly dispersive propagation conditions. The quality of an emulator is of course essentially determined by the precision of the underlying channel model. Unfortunately, until now no appropriate models existed for the very special power traction systems of rapid transit railways in local transportation systems.

The most general form for the input–output relationship of a continuous-time linear and time-variant (LTV) channel with additive noise is [5], [6]

$$r(t) = \int_{-\infty}^{+\infty} h(\tau, t)s(t-\tau)d\tau + n(t) \tag{5}$$

where $s(t)$ and $r(t)$ are the channel input and output signals, respectively, while $h(t,\tau)$ is the channel's impulse response and $n(t)$ denotes the noise. All real channels and signals have essentially a finite number of degrees of freedom due to restrictions on time duration, fading rate, bandwidth, etc. These restrictions allow to construct a simplified channel model, taking some constraints into account [5], [7]. Although our channel is actually deterministic, its behavior from the receiver's point of view is unknown. Thus, $h(t,\tau)$ can be described by a random process. The channel properties, such as Doppler power density spectrum, delay spread, and amplitude distribution were identified by simulations with the deterministic model in Section III, and are now used here as inputs to develop a novel stochastic model.

A. Classification of Distortions

All channel distortions can be divided into two main classes: continuous and discontinuous distortions.

If the transfer function exhibits no abrupt changes, one speaks of continuous distortions. Generally, for continuous distortions, a difference is made between stochastic and deterministic ones. Stochastic distortions include the fast-fading effects discussed above, while deterministic distortions are caused by long-term fading and the low-pass behavior of the channel. Long-term fading includes fluctuations of the average signal power. Such fluctuations can be caused by the network structure, particularly by rings.

Discontinuous distortions are caused by switching events in an MT-PLC channel, e.g., at turnouts or by connecting a new power consumer. They affect not only the signal attenuation characteristics, but also the complete fast-fading scenario.

B. Discrete-Time Channel Model

The driving force behind time-discrete description of the channel is the development of a model suitable for simulation with modern digital signal processing equipment. In preparation of our approach, some constraints have to be considered.

In general, the duration of a continuous-time impulse response is infinite. Assuming, however, that the energy of any impulse response of a real channel is limited, one may assert that there is always a point on the time axis, for which

$$\int_{T_h}^{\infty} |h(\tau)|^2 d\tau < \varepsilon \tag{6}$$

holds, for an arbitrary small value ε. If ε is sufficiently small, one may limit the duration of channel impulse response at a corresponding T_h value. This assumption allows to define any multipath channel as a channel with finite memory with $h(\tau) = 0$ for $\tau > T_h$. Due to the low-pass character of our channel, the same assumption can be made to restrict the frequency range of the transfer function [22]. Thus, the MT-PLC channel is time and frequency limited. These two fundamental limitations allow to proceed with a time-discrete description, where the continuous-time impulse response is sampled at a certain frequency. Since the duration of the impulse response is time-limited, the necessary amount L of samples is also finite. The channel emulator can then be implemented by means of a complex finite impulse response (FIR) filter with slowly time-variant coefficients [28]. For the final model implementation, some further simplifications are necessary. The time-variant impulse response can be written as a sum of multipath contributions in the form

$$h[n,m] = \alpha[m] \sum_{i=1}^{L_{Pf}} [\alpha_{Pf,i}[m] * h_{TP,i}[n,m]] \tag{7}$$

where $\alpha_{Pf,i}(m)$ represents the time-variant attenuation of the respective path, and $\alpha(m)$ describes the time-varying average

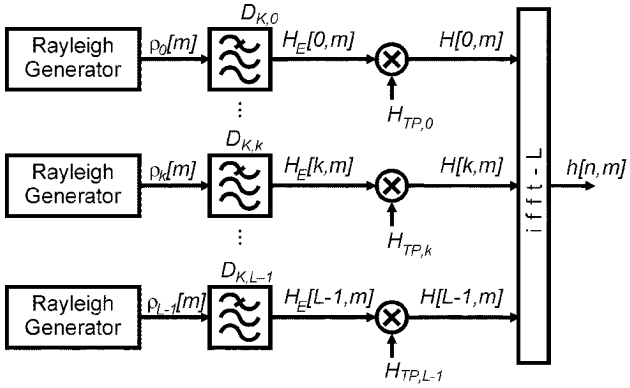

Fig. 12. Structure of the simulation model.

power. The low-pass portion $h_{TP,i}$ depends on length and configuration of the path i, and must thus be individually specified for each path. By extensive investigations of different channels in [18], it could be confirmed, that a single typical low-pass character given by

$$h[n,m] = \alpha[m] \left[\sum_{i=1}^{L_{Pf}} \alpha_{Pf,i}[n] \right] * h_{TP}[n] \tag{8}$$

can be accepted unchanged for all paths. In the frequency domain, we have, respectively

$$H[k,m] = \alpha[m] \cdot H_E[k,m] \cdot H_{TP}[k] \tag{9}$$

where $\alpha[m]$ describes the long-term fading effect, $H_E[k,m]$ the fast-fading effect, and $H_{TP}[k]$ the low-pass characteristic, respectively. (9) allows to separate the influences of the different channel properties on signal propagation and to model them independently.

Since the Doppler spread D_K depends on carrier frequency, our PLC channel exhibits a very specific property. The fluctuation of the received amplitude becomes faster with growing frequency. Consequently, the Doppler spreads for two stochastic processes $H_E[k,m]$ and $H_E[k+1,m]$ are different and increase with rising k. Due to this property, the computation of FIR filter coefficients in the time domain becomes very complicated. In order to be able to implement the amplitude fluctuation effects for different frequencies in the desired way, the calculation of the filter coefficients in the frequency domain appears advantageous. An appropriate model structure for the frequency range up to 500 kHz is shown in Fig. 12.

The general idea behind the channel model discussed here is the description of time-varying channels with memory in form of a set of independent narrowband channels without memory in the frequency domain. The samples of the transfer function are represented by independent stochastic processes and are produced with random number generators. In a further step, filtering is performed with an appropriate low-pass filter representing the Doppler psd. To implement the low-pass characteristic, multiplication coefficients denoted as $H_{TP,k}$ are introduced. The discrete values of the transfer function are equal to the continuous transfer function at certain sampling points in the frequency domain. As it is demonstrated in [22], the absolute position of such frequency points is insignificant. The distance between neighbors, however, has to remain constant and equal to 1/2 of the channel's coherence bandwidth.

The number of samples of the transfer function depends on the duration of the impulse response. If the discrete impulse response with length L has to be computed, then L samples of the transfer function must be generated, which are equidistantly distributed over the frequency range between DC and the sampling frequency.

To implement the convolution of the input signal with channel's impulse response, two mathematical techniques are available, namely, direct convolution in the time domain or multiplication in the frequency domain [21]. The convolution of two signals in the frequency domain using fast Fourier transform (FFT) supposes block by block processing of an infinite input sequence $s[n]$. According to [17], the channel filter taps must be computed at least 32 times faster than the desired fading rate of the channel. Taking slow channel fading into account, the calculated transfer function may be repeated for many blocks of the input signal. This leads to significant simplification of the computational complexity [22].

C. Simulation Results

In this section, some numerical results computed by the simulation model are presented. The time-varying channel transfer function without discontinuous distortions for various but constant receiver movement velocities is generated. The investigated frequency range is 50–500 kHz and the sampling frequency has been fixed to 1.5 MHz. Black areas in Fig. 13 correspond to small amplitudes and white ones to high amplitudes. The channel transfer function $H(f,t)$ is changing over time and frequency, exhibiting the following dominant properties.

1) The speed of amplitude fluctuations increases with frequency. The amplitude fluctuations over time are depending on the Doppler filters D_K, and are selectable over wide ranges. With linear increase or decrease of cutoff frequencies D_K of all filters, practically any receiver velocity of interest can be simulated. Cutoff frequencies equal to zero correspond to channels with static transfer functions.
2) One recognizes that channel transfer functions are highly correlated over certain time and frequency intervals. The width of correlation intervals corresponds to the width of the Doppler spectrum and the number of independent white Gaussian noise generators (WGNG).

V. Analysis of the Channel Specific Requirements for System Design

The scope of applications for MT-PLC primarily comprises automation services. Therefore, the following requirements have to be fulfilled by a communication system:

- data rates up to some 10 kbits\s;
- unrestricted real-time capability;
- high reliability in terms of low bit-error rates;
- robustness against noise and distortions;

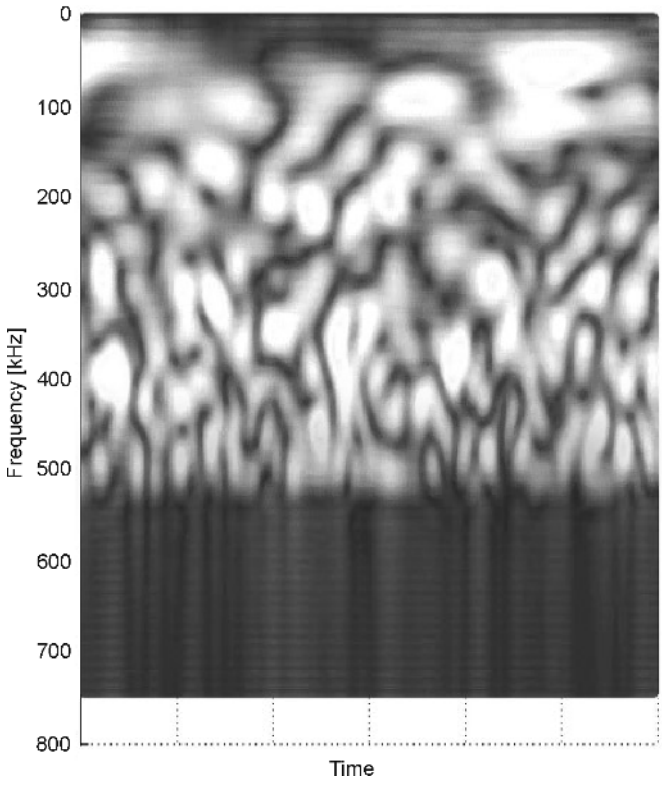

Fig. 13. System transfer function over time and frequency.

- high reliability through permanent availability of communication links;
- multiple access.

The constraints imposed on the design of PLC systems are to a great extend defined by rules of electromagnetic compatibility (EMC). Current norms do, however, not provide clear guidelines with respect to the use of power traction networks in MT as fast digital communication links. Therefore, no proper definition of limits, e.g., concerning allowable transmission psd can be given. To determine potentialities of MT-PLC channels, studies about electromagnetic emissions from power traction networks are inevitable. Some respectable work has been done in [19] with focus on radiated emissions from power lines in urban areas. [19] presents the derivation of a so-called coupling factor, which enables the characterization of radiated electromagnetic fields in dependence of signal power injected into lines. Because of significant uncertainties with respect to limits of injected signal power into MT-PLC channels, the following investigations are made without specifying absolute power values, but using the signal-to-noise ratio (SNR) instead.

A. Synchronization Based on Noise Impulses

In this section, the channel capacity is estimated, considering the constraints imposed by a limited frequency band, limited signal power, and the typical noise scenario of the channel.

Investigating the noise scenario in Section II revealed that background noise and periodic impulsive noise have substantial influence on channel characteristics with respect to communications. While the background noise is continuously present, the impulsive disturbances occur only as long as traction current flows through the rectifier. In the time interval between impulsive bursts and between individual impulses no significant disturbances are present, except the background noise. Hence, the synchronization of information signals with noise impulses appears advantageous, so that communication takes only place between such noise impulses. In this way, the necessary injected signal power could be significantly reduced. For a rough analysis of channel capacity and the benefit, which could be obtained by synchronization with noise impulses, two sample channels are compared, one being synchronized as mentioned above, while the other does not care for the noise impulses.

For the communication system without synchronization on impulses, it is assumed that the channel is permanently impaired by impulsive noise. The psd of such noise is typically approximately 30 dB higher than the background noise in the whole frequency range under consideration. The channel is available 100% of time. Thus, there are no time intervals excluded from data transmission.

When, on the other hand, synchronization with the noise impulses is implemented, nothing but the background noise is present during the available transmission intervals. These intervals are now, however, substantially reduced. If the duration of a typical impulse is assumed to be 0.5 ms, then the total relative time span affected by noise impulses for 12-pulse rectifier is given by

$$t_{\text{rel.disturb.}} = \frac{\sum_{i=1}^{N_{\text{imp}}} t_{\text{Imp}}}{T_b} = \frac{\sum_{i=1}^{12} 0.5\ \text{ms}}{20\ \text{ms}} = 0.3. \tag{10}$$

Since an impulse jitter of $t_{\text{Jitter}} = \pm 100\ \mu\text{s}$ must be additionally taken into account, the remaining undisturbed time interval available for communication is reduced to

$$t_{\text{comm}} = 1 - \left(t_{\text{rel.disturb}} + \frac{2 \cdot t_{\text{Jitter}}}{t_{\text{imp.rate}}} \right) = 0.58. \tag{11}$$

For the comparison of both communication systems, Shannon's theory of channel capacity is now used [29], specifying

$$C = \frac{t_{\text{comm}}}{2} \log_2 \left(1 + \frac{S_{\text{Sig}}}{\sigma^2} \right) \tag{12}$$

as the maximal data rate for which error-free transmission would be theoretically possible. Note that the result of (12) is independent of coding or modulation schemes. S_{Sig/σ^2} specifies the SNR.

Fig. 14 eventually shows the data rate comparison for the two proposed systems as a function of the received signal strength related to the background noise, whereby the rates are given in bits per second per Hertz. It is evident that in the case of a synchronized system, the capacity is superior for low received signal power values. The flat course of the curve with synchronization in comparison with the unsynchronized version can

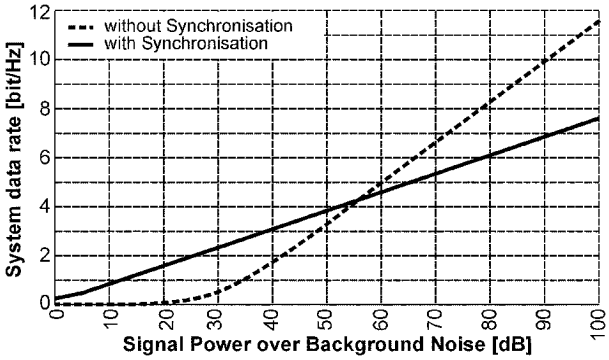

Fig. 14. Synchronization with impulsive noise.

be explained by the restricted time available for transmission. When the SNR exceeds 50 dB, the unsynchronized version is more favorable. It should also be noted, that the implementation of an MT-PLC system without synchronization on noise impulses is less complicated. When the performance of the two variants is equal (at an SNR of 55 dB), we can see from Fig. 6 that the emission is around −30 dBm/Hz, which corresponds to the maximum level of impulsive noise.

Usually, PLC is treated differently from unintentional radiation, compare, e.g., EN 50065-1:2002 and the German NB30. Currently, however, there are no regulations for the use of PLC in railway applications, which have their special norms. Hence, it can be expected, that the applicable limits for the intended application will be below the limits of the railway EMC regulation specified in EN 50121. This means, that the allowable transmission power will in any case be so severely limited, that a synchronized version will exhibit superior performance.

B. Multiple Access

For multiuser communication links, the resources of the channel have to be shared among numerous users. The way in which these limited resources are split between subscribers, namely trains, is crucial for overall system performance and must consider channel properties, as well as requirements concerning acceptable delay times and amounts of data to be transmitted. Real-time requirements for automation tasks call, e.g., for a quasi-continuous data exchange between trains and fixed stations. If inevitable, only very short interruptions are permitted. Thus, it appears advantageous to divide the whole network into several independent logical cells in order to limit the number of subscribers in such a cell and to enable reuse of carrier frequencies.

Within a cell, it is useful to distinguish between three types of multiple access: fixed multiple access [like time-division multiple-access (TDMA) and frequency-division multiple-access (FDMA)], random access, and demand assignment methods [11]. Due to the structure of our network, fixed multiple access appears favorable. Furthermore, a fixed central master can control channel access, while the trains represent slave stations. Data exchange can thus be organized according to robust master–slave principles. The stationary master takes over the tasks of the message distribution from upper level communication networks to the slave stations (downlink), as well as collecting messages from the slave stations within a cell and forwarding them to upper levels (uplink). Each slave needs its own uplink channel, which can be placed into a time and frequency plane.

Note that the frequency range of each uplink must be larger than the coherence bandwidth of the channel defined in Section III, in order to avoid complete signal extinction and to guarantee a certain redundancy.

In addition to the proposed downlink and uplink channels a so-called logical channel is needed, on which a new subscriber, e.g., a train which enters the cell, can announce itself to the associated master.

C. Modulation and Channel Estimation

The goal of modulation is to prepare the digital information for transmission and to construct the appropriate signal coding to consider the channel properties and restrictions in order to exploit the channel as close as possible to its capacity. The highest robustness against low-pass effects and frequency-selective disturbances as well as high-spectral efficiency can be achieved with multicarrier schemes such as orthogonal frequency-division multiplexing (OFDM).

The concept of OFDM is already 28 years old [12]. Due to enormous progress in integrated circuit technology toward fast and complex digital signal processing, OFDM is now widely applied even in classical low-cost areas such as digital audio broadcasting (DAB) or digital video broadcasting (DVB), as well as for digital subscriber lines (DSL). In numerous publications, OFDM has also been suggested as a preferable method for communications over power lines [24], [25].

With OFDM, the information is distributed over a large number of carriers properly spaced apart in the usable frequency range. The special kind of spacing with OFDM provides "orthogonality" which enables perfect carrier detection and separation by demodulators using the well-known correlation principle. With OFDM, the whole available frequency range is divided into a number of independent subchannels. Due to deep notches, which may be caused by multipath propagation, some subchannels can be faded out and become useless for data transmission, so that a sufficiently large redundancy is required. In the frequency domain, such redundancy can be established, e.g., by the method of diversity [26].

Each PLC link of an MT network exhibits its unique profile due to an individual structure, and is additionally time-variant due to the motion of communications nodes. Adaptive transmission schemes promise a higher efficiency than those with constant parameters. To implement appropriate adaptive algorithms requires, however, on one hand, special hardware, and sophisticated channel estimation on the other.

If the impulse response of a channel is known at the receiver, the influence of the channel on a transmitted signal can at least be partially compensated. This compensation procedure is called equalization [6]. For time-variant communication channels, equalization must be able to follow changes of channel

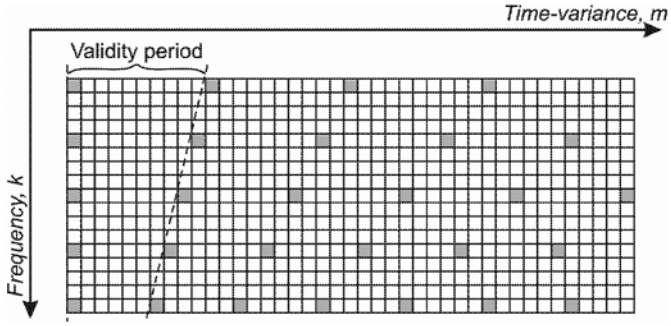

Fig. 15. Channel estimation.

parameters fast enough. There are numerous publications dedicated to appropriate solutions, which are based on the following two basic principles:

1) Usage of additional special estimation sequences, e.g., in the form of pilot signals or PN-sequences (pseudonoise) [20], [27].
2) Estimation of channel parameters using the information bearing signal itself [20].

A combination of both principles is of course also possible.

Here, we will focus on the consequences of channel studies from the sections above, which influence the choice of appropriate equalization algorithms.

In [22], it is shown that a power line channel is symmetrical, i.e., the same transfer function is found in both directions from transmitter to receiver and *vice versa*, only if the access impedances at both communication devices are identical. Unfortunately, this quite simple condition is difficult to fulfill. Under normal operating conditions, the output resistance of a transmitter must be kept as low as possible, due to the low access impedance normally found at the network. Opposite to this requirement, the input impedance of a receiver has to be as high as possible to mitigate its influence on signal propagation. Hence—as channel asymmetry will be the standard situation—the estimation procedure must be performed in both directions independently.

For estimation by means of special sequences a transmitted signal consists of two portions, namely, an information and an estimation part. For time-variant channels, it is essential to find out how frequently estimation must be repeated. The according time span is called validity period and depends on the channel's coherence time defined in Section III. Within the validity period the channel can be considered as time invariant. Since each OFDM subchannel behaves orthogonal, this modulation scheme offers special possibilities of channel estimation. A few subchannels can, e.g., be used for channel estimation, while the others are available for data transfer. The so-called estimation subchannels carry pilots, which are *a priori* known, both by the transmitter and the receiver. The main disadvantage of this procedure is, that the pilots are useless for information transfer, i.e., the useful data rate is reduced. A further reduction may be imposed by strong ingress of broadcast stations, i.e., strongly affected subchannels must be avoided. Optimization of estimation algorithms with sufficient accuracy, low complexity, and moderate reduction of the useful data rate always turns out as a challenging task.

As an example, Fig. 15 shows the result of such an optimized positioning of pilot carriers. Here, a 2-D channel estimation is accomplished. The grey fields mark the pilot carriers, while white fields mark data arrays. In [22] is proven that an impulse response of the length L can be completely determined by L pilot carriers. The absolute position of the carriers is irrelevant, they must, however, be placed equidistantly over in the whole frequency range of interest. The values of the transfer function between the pilot carriers can be approximated using suitable interpolation algorithms (Fourier transform, Wiener interpolation, etc.). As MT-PLC channels exhibit extreme wideband nature, the validity period varies from carrier frequency to carrier frequency. Since at low frequencies the validity period is longer, the pilot carrier spacing may be extended there. This way, the overall number of pilots can be minimized.

An important advantage of pilot-based channel estimation in the comparison with conventional estimation, based, e.g., on PN-sequences, is that the actual channel transfer function is permanently available without noticeable reduction of the useful data rate. A disadvantage of the proposed 2-D approximation is that abrupt changes of the channel transfer function within an approximation period can lead to incorrect interpolation, causing incorrect reception of all symbols falling into this period.

VI. Conclusion

Extended rail-based local transportation systems represent important traffic backbones of almost any major city in the world. Current MT systems suffer, however, from a lack of reliable and permanently available communication links. Wireless solutions have turned out as infeasible in most cases, due to the fact that significant portions of MT systems are underground. Thus, PLC over the existing power supply lines can be regarded as a rewarding approach. MT networks are, however, very different from usual electricity supply systems, i.e., they are DC-powered, one of the conductors is the rail itself, while the other may be a "third rail" or an overhead wire. Furthermore, caused by the rectifiers, a very peculiar noise scenario is found. Obviously, both the usage of exiting models and communication equipment for conventional PLC channels would not be feasible here. Therefore, the work reported in this paper, had to focus on channel investigation and modeling in order to develop novel adapted solutions. Various new ideas for proper PLC signal injection had to be investigated, as well as network conditioning methods. As a result, a complete MT channel model is now available, including peculiar properties such as the behavior of ring structures, as well as the impact of the Doppler effect invoked by moving trains, and last but not least the very special interference scenario found in these DC environments. In addition, discussions of PLC channel coherence bandwidth and ultra-wideband phenomena represent novelties which were not studied before at conventional power lines.

Eventually, this paper presents clear guidelines for building emulation hardware, so that no further expensive field trials in harsh and not easily accessible environments are needed. Channel adapted PLC system design for power traction networks of MT can now be successfully started.

ACKNOWLEDGMENT

The authors wish to express their gratitude to the "Verkehrsaktiengesellschaft" in Nuremberg and the "Kölner Verkehrsbetriebe" in Cologne, both Public Transport Authorities in Germany, for their contributions to this investigation. They would also like to express special thanks to Prof. D. Korobkov for his counseling assistance during this work.

REFERENCES

[1] G. Griepentrog, "Powerline communication on 750 V DC networks," in *Proc. 5th Int. Symp. Power Line Commun. Appl.*, 2001, pp. 259–264.
[2] J. Rupp, G. Griepentrog, and P. Karols, "Modeling of the signal transmission characteristics of power lines for local transportation systems," in *Proc. 7th Int. Symp. Power Line Commun. Appl.*, 2003, pp. 148–153.
[3] H. Brand, *Schaltungslehre linearer Mikrowellennetze*. Stuttgart, Germany: S. Hirzel Verlag, 1970, ISBN 3-777-60 010-5.
[4] H. Meyr and M. Moenecleay, *Digital Communication Receivers*. New York: Wiley, ISBN 0-471-50 275-8.
[5] P. Bello, "Characterization of randomly time-variant linear channels," *IEEE Trans. Circuits Syst.*, vol. CS-11, no. 4, pp. 360–393, Dec. 1963.
[6] J. Proakis, *Digital Communications*. New York: McGraw-Hill, ISBN 0-07-232 111-3.
[7] T. Kailath, Sampling models for linear time-variant filters MIT Research Lab. Electron., Cambridge, MA, Rep. 352, May 25, 1959.
[8] J. D. Gibson, *Communications Handbook*. Piscataway, NJ: IEEE Press, ISBN 0-84 938 349-8.
[9] H. Schulze, "Digital Audio Broadcasting: Das Übertragungssystem im Mobilfunkkanal," in *Ausarbeitung für ein Seminar*, Meschede, Sep. 1995, vol. 19, no. 21.
[10] J. Perl, A. Shpigel, and A. Reichman, "Adaptive receiver for digital communication over HF channels," *IEEE J. Sel. Areas Commun.*, vol. SAC-5, no. 2, pp. 304–308, Feb. 1987.
[11] H. Bischl, "Analyze, Optimierung und Vergleich von Kanalmodellen für Vielfachzugriffssysteme und zugehörige Protokolle," *VDI*, 1995, Reihe 10, Nr. 341.
[12] S. B. Weinstein and P. M. Ebert, "Data transmission by frequency division multiplexing using the discrete Fourier transform," *IEEE Trans. Commun.*, vol. 19, pp. 628–634, Oct. 1971.
[13] D. C. Cox, "910 MHz urban mobile radio propagation: Multipath characteristic in New York City," *IEEE Trans. Commun.*, vol. 21, no. 11, pp. 1188–1194, Nov. 1973.
[14] M. Faili, Ed., Digital land mobile radio communications—COST 207, Final Rep., Commission of the European Community, Luxembourg, 1989.
[15] M. Arzberger, K. Dostert, T. Waldeck, and M. Zimmermann, "Fundamental properties of the low voltage power distribution grid," in *Proc. Int. Symp. Power Line Commun. Appl.*, Essen, Germany, Apr. 1997, pp. 45–50.
[16] W. Furman and J. Nieto, "Understanding HF channel simulator requirements in order to reduce HF modem performance measurement variability," in *Proc. HF01, the Nordic HF Conf.*, Aug. 2001.
[17] *STANAG 4285*, Characteristics of 1200/2400/3600 bits per second single tone modulators/demodulators for HF radio link, North Atlantic Treaty Organization, Brussels, Belgium, 1989.
[18] M. Goetz, "Mikroelektronische, echtzeitfähige Emulation von Powerline-Kommunikationskanälen," Ph.D. dissertation, Berlin, Germany, 2003, Mensch&Buch Verlag.
[19] M. Gebhardt, "Emission elektromagnetischer Felder aus Energieversorgungsnetzen durch hochfrequente Kommunikationssignale," Ph.D. dissertation, Berlin, Germany, 2003, Mensch&Buch Verlag.
[20] D. Korobkov, S. Portnoj, and V. Zjablov, *High Speed Data Transmission in Real Channels*. Moscow: Radio and Communication, 1991.
[21] J. Proakis and D. Manolakis, *Digital Signal Processing: Principles, Algorithms and Applications*. Englewood Cliffs, NJ: Prentice-Hall, 1996.
[22] P. Karols, *Nachrichtentechnische Modellierung von Fahrleitungsnetzen in der Bahntechnik*. Berlin, Germany: Mensch&Buch Verlag, 2005.
[23] H. Linder, H. Bauer, and C. Lehmann, *Taschenbuch der Elektrotechnik und Elektronik*. Leipzig: Carl-Hanser-Verlag, 1998.
[24] L. Lampe and J. Huber, "Bandwidth efficient power line communications based on OFDM," *AEÜ Int. J. Electron. Commun.*, vol. 54, no. 1, pp. 2–12, 2000.
[25] M. J. Galda, "An experimental OFDM-modem for CENELEC B-band," in *Proc.f HF01, The Nordic HF Conf.*, Aug. 2001.
[26] T. Waldeck, "Einzel- und Mehrträgerverfahren für die störresistente Kommunikation auf Energieverteilnetzen," Ph.D. dissertation, Berlin, Germany, 2000, Logos Verlag.
[27] Y. Bar-Ness, U. Spagnolini, and O. Simeone, "Pilot based channel estimation for OFDM systems by tracking the delay-subspace," *IEEE Trans. Wireless Commun.*, vol. 3, no. 1, pp. 315–325, 2004.
[28] C. C. Watterson, Experimental Confirmation of an HF channel model, ESSA Tech. Rep., ERL 112-IST 80, 1968, (NTIS Order No. AD699-468).
[29] C. E. Shannon, "A mathematical theory of communication," *Bell Syst. Tech. J.*, vol. 27, pp. 279–423, 1948.

Pavels Karols received the Degree in electric power engineering from the Riga Technical University, Riga, Latvia, in 2000.

From 2000 to 2004, he was a Research Assistant at the Institute of Industrial Information Technology, University of Karlsruhe, Karlsruhe, Germany. Presently, he is with Siemens AG Power Transmission and Distribution, Erlangen, Germany.

Klaus Dostert (SM'96) received the M.S. degree from RWTH Aachen, Germany, in 1976, and the Ph.D. degree from the University of Kaiserslautern, Kaiserslautern, Germany, in 1980.

During the following years, he worked as a Postdoctoral Fellow in the fields of RF communications, signal processing, and data transmission over power lines. In 1992, became a Full Professor at the University of Karlsruhe. In 2000, he was a Guest Lecturer on PLC at the Technical University of Vienna. During the past 13 years, his work was focused on PLC, including channel emulation, system design, and EMC. He has published more than 120 scientific papers and two books on power line communications.

Gerd Griepentrog received the Degree in automation engineering from the former Institute of Technology, Zwickau, Germany, in 1993 and the Ph.D. degree in electrical engineering from the Technical University, Chemnitz, Germany, in 1996.

Since 1996, he has been with Siemens AG Corporate Technology, Erlangen, Germany, and is currently Head of the Power Management Department.

Simon Huettinger received the Dr. Ing. degree from the University of Erlangen–Nuernberg, Germany, in 2003.

From 2000 to 2003, he was with the Institute for Information Transmission, University of Erlangen–Nuernberg. Presently, he is with Siemens AG Corporate Technology, Erlangen, Germany.